Tunable optical absorption on "ZnxTixO4-3yN2y" nanosized spinel powders

David Berthebaud, Fabien Grasset, Vincent Allegret-Maret, Soraya Ababou-Girard, Stanislav Pechev

Tunable Optical Absorption on "$Zn_xTi_xO_{4-3y}N_{2y}$" Nanosized Spinel Powders

David Berthebaud,[†] Fabien Grasset,*[,†] Vincent Allegret-Maret,[†] Soraya Ababou-Girard,[‡] and Stanislav Pechev[§]

Science Chimiques de Rennes, UMR 6226 CNRS-Université de Rennes 1, Campus de Beaulieu, CS74205, F-35042 Rennes Cedex, France, PALMS, UMR CNRS-UR1 6627, Université de Rennes 1, Campus de Beaulieu, 35042 Rennes Cedex, France, and Institut de Chimie de la Matière Condensée de Bordeaux, UPR CNRS 9048, Université Bordeaux-1, 87 Avenue du Dr Albert Schweitzer, F-33608 Pessac Cedex, France

Received: February 28, 2007; In Final Form: March 29, 2007

Using a recently developed sol−gel route to prepare new Ti^{4+}@ZnO nanocolloids, we were able to synthesize, at relatively low temperature (maximum 750 °C) and very short annealing time (1 h) under ammonia gas flow, nanosized colored "$Zn_{1.33}Ti_{1.33}O_{4-3y}N_{2y}$" oxynitride powders (Zn/Ti = 1) with tunable optical absorption. Above the dissociation temperature of ammonia, the UV−vis spectra are progressively red-shifted with increasing nitriding temperature and the nanosized powder shows a yellowish color at 700 °C under NH_3. X-ray diffraction, scanning electron microscopy, X-ray photoemission spectroscopy, oxygen and nitrogen analysis, and UV−vis spectroscopy measurements show that this red shift is directly related to the nitrogen content.

Introduction

Nanomaterials represent a new class of materials with continuously increasing fields of application−environment, catalysis, biotechnology, and magnetic and optical devices. Particularly, nanoparticles have generated a large research effort in the past 10 years because their properties differ markedly from those of their bulk counterpart.[1] Recently, we developed a new low-cost colloidal sol−gel route to prepare nanosized colored "ZnTiON", 1 μm thick, porous layers on glass.[2] First, we had prepared highly concentrated ZnO nanocolloids using an alcoholic clusters route developed in refs 3 and 4. Then we added titanium tetraisopropoxide in order to obtain new Ti^{4+}@ZnO nanocolloids. To get colored oxynitrides, we used an ammonia-induced replacement of oxygen by nitrogen according to the general equation oxide + NH_3 → oxynitrides + H_2O, well-known from classical solid-state chemistry.[5] These kinds of colored porous thin films showed excellent photostability and photodegradation of an aqueous methylene blue solution in the visible spectrum.[2,6] These results corroborate recent works about oxynitrides or nitrogen-doped oxides reporting high photocatalytic activity under visible light (refs 7 and 8 and references therein). In this paper, we present the microstructural characterization of "ZnTiON" nanosized powders obtained from nanocolloids. The nanosized powders were studied by X-ray diffraction (XRD), scanning electron microscopy (SEM), X-ray photoemission spectroscopy (XPS), oxygen and nitrogen analysis, and UV−vis spectroscopy.

Experimental Section

Synthesis Process. The nanosized powders were synthesized from Ti^{4+}@ZnO nanocolloids by evaporation of alcohol using a rotating evaporator. Briefly, Ti^{4+}@ZnO nanocolloids were prepared using zinc acetate dihydrate (4.39 g) suspended in *n*-propanol (40 mL) under ambient atmosphere and distilled for 10 min in a preheated silicon oil bath (125 °C). Under magnetic stirring, methanolic tetramethylammonium hydroxide (TMAH) base solution was rapidly added (9 mL, 2.37 M) to the still hot precursor (45 °C), yielding initially a turbid precipitate which next turned into a clear nanocolloid after a few minutes. To the fresh sol, we added titanium tetraisopropoxide precursor (Zn/Ti = 1), which readily reacts with the ZnO nanocrystals. After cooling to room temperature, the solvant was removed using a rotary evaporator (40 °C, 20 Pa). The resulting soft-gel was then kept in an oven at 100 °C during 1 week in order to solidify, then was ground and pre-sintered at 400 °C in air to remove the organic residues, and finally transformed into white powder. To get colored oxynitrides, the powders (0.5 g) are annealed under ammonia gas (purity N36) for 1 h at temperatures between 550 and 750 °C and then cooled by removing the electrical power under ammonia flow.

Elemental Analysis. Nitrogen and oxygen contents were determined with a TC-436 analyzer from LECO, Inc. using the inert gas fusion method, nitrogen as N_2 by thermal conductivity, and oxygen as CO_2 by infrared detection. The apparatus was calibrated with N_2 and CO_2 gas (purity, 99.95%). At least three analyses were performed for each sample in the same conditions.

X-ray Intensity Measurements and Peak Profile Analysis. The powder X-ray diffraction data were recorded at diffractometers with Bragg−Brentano geometry, Cu Kα radiation (40 kV, 30 ÷ 40 mA, and 0.5 ÷ 10 s integration time), proportional detectors, and secondary monochromators. At room temperature a Philips PW 3020 was used. The high-temperature XRD experiments were performed on a Philips X'Pert MPD with an Anton Paar HTK-16 camera, where the powder sample is deposed directly on the heating element−a platinum strip.

The average apparent crystallite size (ϵ_β) was evaluated from a whole diffraction pattern profile analysis, using last developments implemented in the Fullprof program (version 2.0 Nov 2001, LLB, Juan Rodriguez-Carvajal). A normalized Voigt

* To whom correspondence should be addressed. Telephone: +33 223 236 540. Fax: +33 223 236 799. E-mail: grasset@univ-rennes1.fr.
[†] UMR 6226 CNRS, Université de Rennes 1.
[‡] UMR CNRS-UR1 6627, Université de Rennes 1.
[§] Université Bordeaux-1.

10.1021/jp0716334 CCC: $37.00
Published on Web 00/00/0000 PAGE EST: 5.1

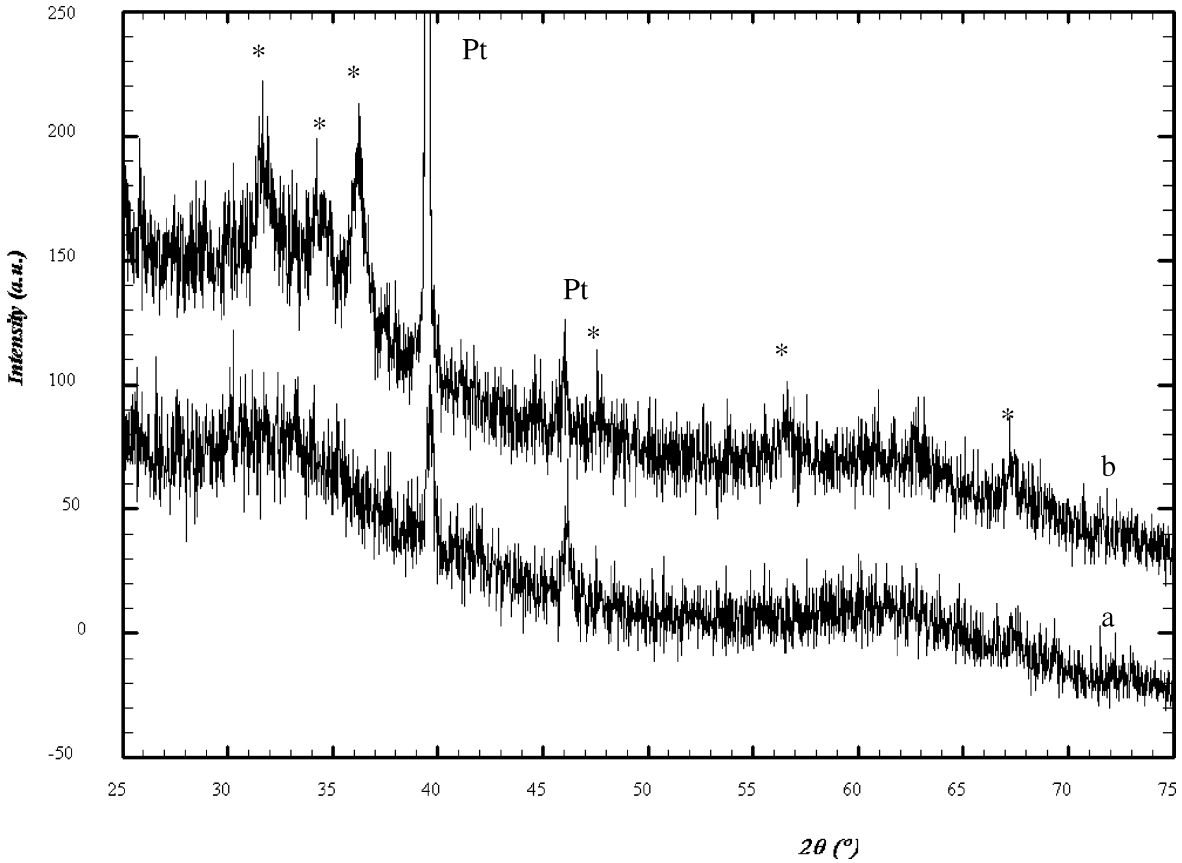

Figure 1. X-ray diffraction at 25 °C of nanopowders with Zn/Ti = 1 (a) and Zn/Ti = 2 (b) ratios. (Pt = platinum sample holder; ∗ = ZnO main peaks.)

function (convolution of Gaussian and Lorentzian functions) was used to fit the peak profiles. The profile analysis is based on the angular dependence of the full width at half-maximum (FWHM) of the Gaussian and Lorentzian components (H_G and H_L, respectively). Both instrumental and sample intrinsic contributions to the line broadening were examined separately. When the instrumental resolution function (IRF) is known, the sample contribution to the line profile is calculated as follows:

$$H_G^2 = (U_{\text{strain iso}} + (1-\xi)^2 D_{\text{strain aniso}}^2) tg^2\theta + \frac{G_{\text{size iso}}}{\cos^2\theta}$$

$$H_L = (X_{\text{strain iso}} + \xi D_{\text{strain aniso}}) tg\theta + \frac{Y_{\text{size iso}} + F_{\text{size aniso}}}{\cos\theta}$$

where $U_{\text{strain iso}}$, $X_{\text{strain iso}}$, $G_{\text{size iso}}$, and $Y_{\text{size iso}}$ are refinable parameters related to isotropic size and strain effects on the line broadening, while $D_{\text{strain aniso}}$ and $F_{\text{size aniso}}$ are analytical functions for an *hkl*-dependent broadening model. ξ is a mixing coefficient for the Lorentzian part of the strains. The integral-breadth method is applied, finally, to determine the crystallite size and strains in the sample. "Perfect" Y_2O_3 powder was used as a standard to determine the resolution function of the diffractometer. The observed line broadening was modeled by considering isotropic size and strain contributions. Only the size-related terms of H_G and H_L ($G_{\text{size iso}}$ and $Y_{\text{size iso}}$) converged to significant values. The strain-dependent parameters ($U_{\text{strain iso}}$ and $X_{\text{strain iso}}$) had meaningless values, which did not influence the profile fitting of the XRD patterns. After the profile refinement, the apparent size along each reciprocal lattice vector is calculated. The average apparent crystallite size (ϵ_β) can be related to the true size, but only if the crystallite shape is known or assumed. For instance, for a spherical crystallite, the true diameter D is simply given by $4/3(\epsilon_\beta)$. Moreover, this simple relation is strictly valid for a monodisperse system.[9] So, the true size could be defined only in the case of single-domain nanoparticles without amorphous shell, as it is for transmission electron microscopy (TEM) and/or scanning electron microscopy (SEM) images.

Morphological Investigations by SEM. SEM photographs were taken by JEOL JSM 6301F microscope to examine the shape and size of the nanoparticles.

UV−Vis Spectroscopy. Diffuse reflectance spectra were collected using a UV−vis CARY 100 spectrometer equipped with a Labsphere DRA-CA-30I with a 70 mm diameter coated with Spectralon (PTFE). The absolute reflectance of the sample is compared with a calibrated 2 in. D 99% Spectralon reflectance standard.

X-ray Photoemission Spectroscopy. XPS was performed under a base pressure of 5×10^{-9} mbar using a VSW HA100 spectrometer. The analyzer was operated with at constant pass energy of 22 eV, which leads to an experimental resolution of 1.1 eV. The X-ray source used either Al or Mg Kα excitation radiation at 1486.6 and 1283.6 eV, respectively. The spectrometer binding energy scale was initially calibrated against the Au 4f7/2 (84.0 eV) level and Cu 2p3/2 (932.7 eV). Since the films were nonconductive, they were referenced to adventitious hydrocarbon with C1s binding energy at 284.9 eV

Results and Discussion

Using the described soft method to synthesize ZnO nanocolloids, the hydrodynamic diameter of the ZnO nanoparticles is around 7 nm.[10] Nevertheless, analysis of the X-ray powder

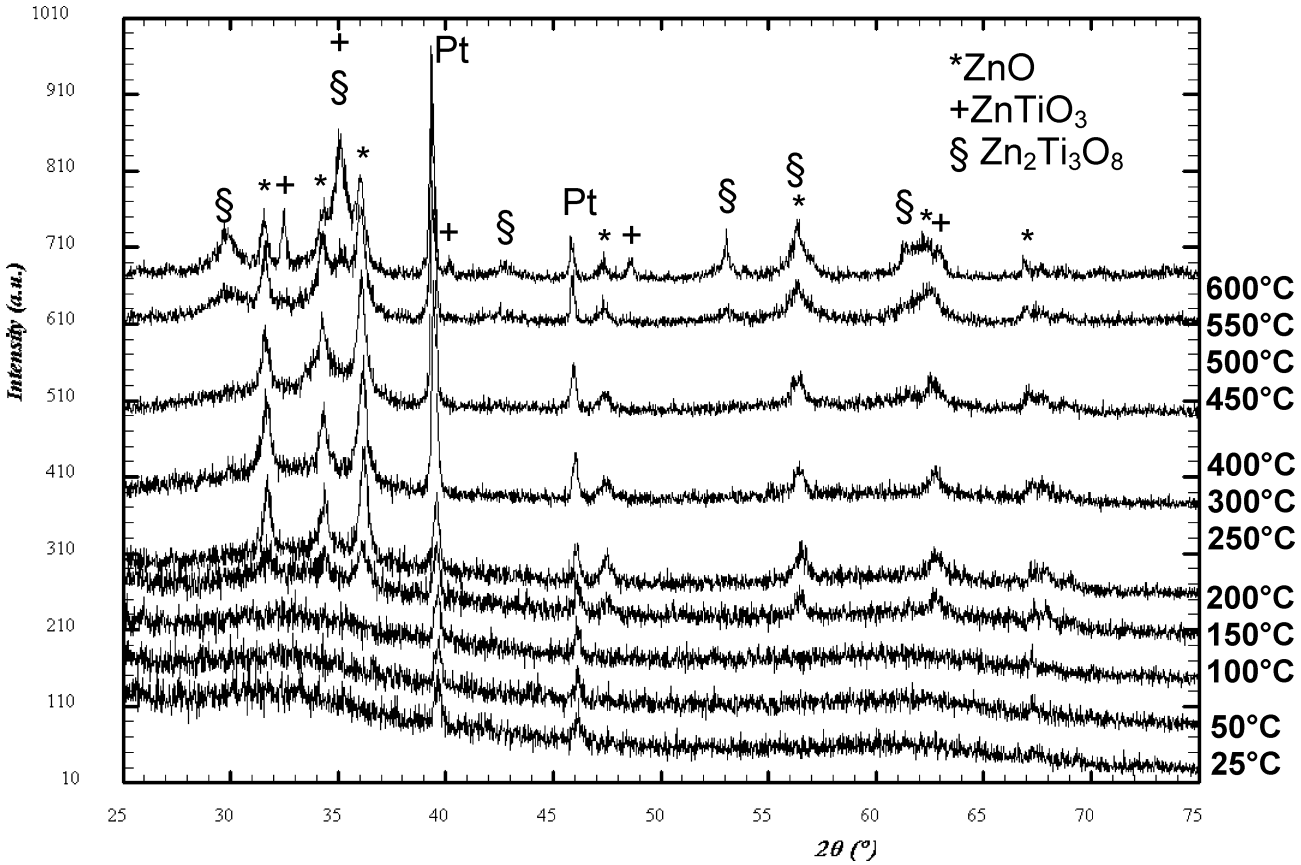

Figure 2. Temperature-dependent X-ray diffraction under air atmosphere.

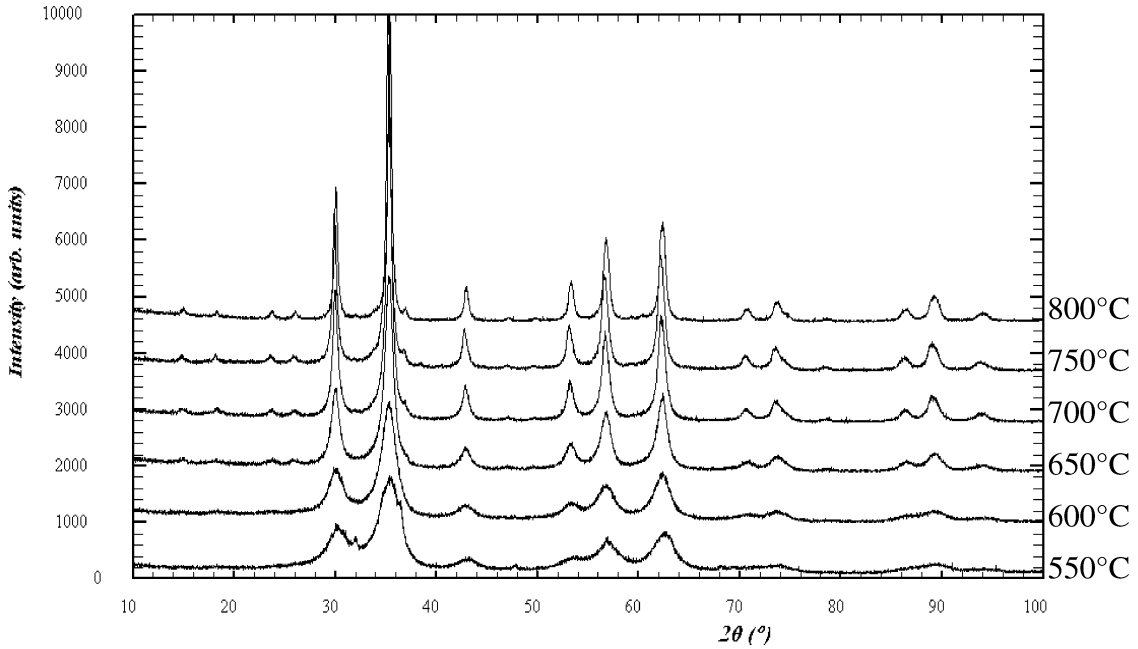

Figure 3. XRD patterns of "ZnTiON" oxynitrides powder.

diffraction data of the Ti@ZnO solid gel obtained after removing the alcohol show amorphous structure (Figure 1).

This amorphous structure can be explain by the fact that Ti^{4+} tetraisopropoxide (i) partly decomposes the ZnO nanocrystals (this has been confirmed by XRD in this work and in complementary UV−vis absorption and DLS measurements in our previous work[10]); (ii) forms itself into amorphous compounds at room temperature. In fact, XRD data reveal that the decomposition of ZnO nanoparticles is dependent on the amount of titanium tetraisopropoxide added into the ZnO nanocolloids. In Figure 1, the X-ray patterns of two different Zn/Ti ratios are represented. We notice that the peaks of ZnO appear with the ratio Zn/Ti = 2, whereas they are not present for the Zn/Ti = 1 ratio.

In situ temperature-dependent X-ray diffraction in air shows that above 150 °C, for the Zn/Ti = 1 ratio, peaks of zinc oxide appear again (Figure 2). The binary compounds in the system Zn−Ti−O can be detected only at 500 °C, and no pure phase

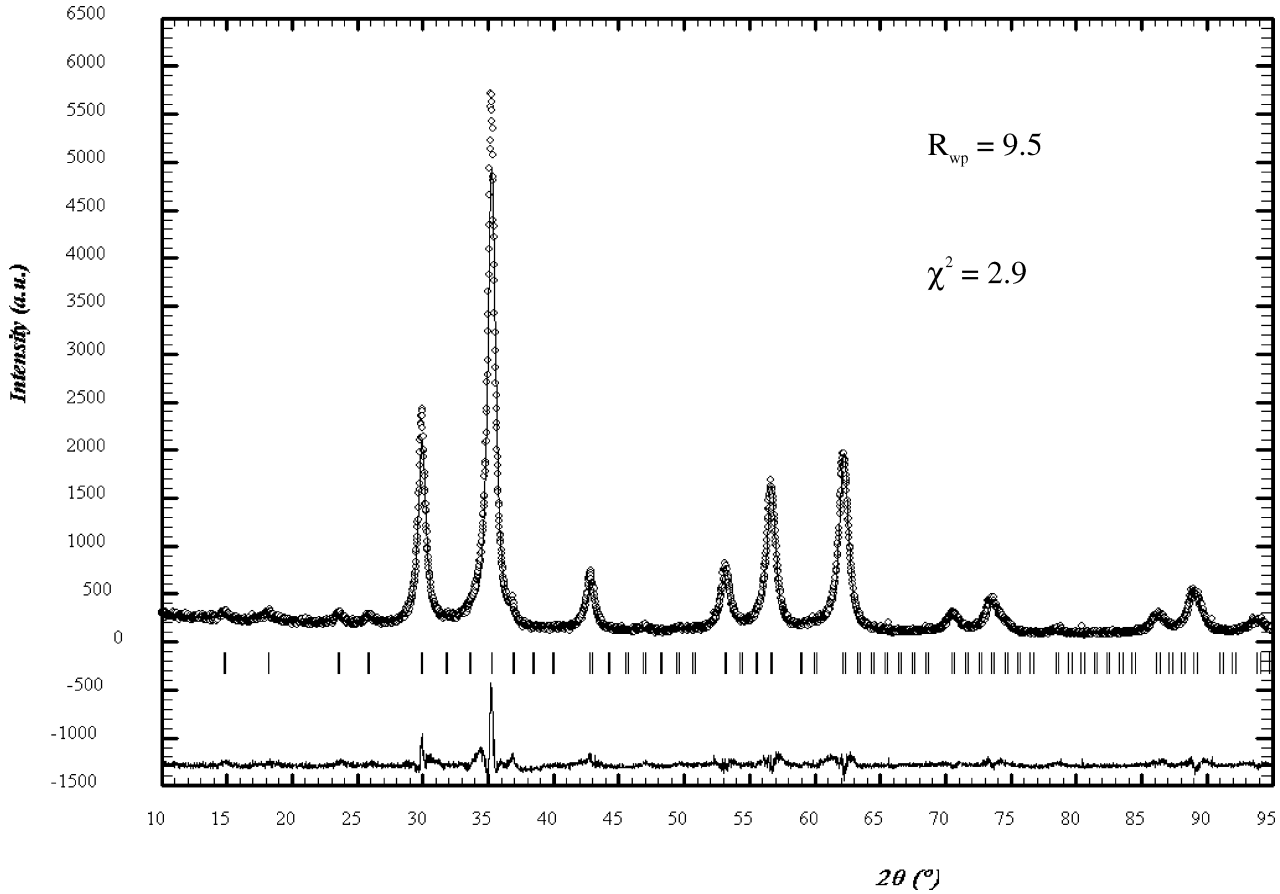

Figure 4. Observed, calculated, and difference X-ray diffraction profiles for the compound annealed at 750 °C.

TABLE 1: LECO Analysis and XRD Results

temp (°C)	O (wt %)	N (wt %)	cell param (nm)	chem composn[a]	$\epsilon_{\beta\,(nm)}$
600 (NH_3)	27.7	1.8	8.430(1)	$Zn_{1.33}Ti_{1.33}\square_{0.33}O_{3.65}N_{0.24}\square_{0.11}$	4.2(5)
650 (NH_3)	25.9	2.5	8.430(1)	$Zn_{1.33}Ti_{1.33}\square_{0.33}O_{3.49}N_{0.34}\square_{0.17}$	7.3(5)
700 (NH_3)	24.9	3.0	8.441(1)		11.0(5)
750 (NH_3)	23.8	3.6	8.441(1)		14.3(5)
800 (NH_3)	25.8	2.5	8.438(1)		15.4(5)

[a] Taking the density into account. □ represents vacancy.

could be prepared in air until 600 °C. The presence of $ZnTiO_3$ (JCPDS card n° 26-1500) and $Zn_2Ti_3O_8$ phases as impurity agrees with the Zn−Ti−O phase diagram.[11] X-ray diffraction under ammonia atmosphere with our laboratory apparatus was not possible because of the high activity of ammonia gas. Only pure phases were prepared from annealed solid-gel (i) at 400 °C in air and (ii) using ammonia atmosphere with a temperature higher than 550 °C (Figure 3).

Analysis of the room-temperature X-ray powder diffraction data indicates that "ZnTiON" compounds annealed between 600 and 750 °C are isostructural with a cations deficient spinel type structure such as $Zn_2Ti_3O_8$ ($a = 8.390$ Å).[13] The observed XRD patterns were refined using the Le Bail method. The refined values of the lattice parameters and the average apparent crystallite size (ϵ_b), extracted from the line profile fit are given in Table 1.

The observed, calculated, and difference X-ray diffraction profiles for the compound annealed at 750 °C are shown as examples in Figure 4. Classically, $Fd\bar{3}m$ is used as the space group for spinel type structure, but the defect spinel that exhibits ordered cation vacancies should be indexed with $P4_132$.[12,13] This ordering leads to a space group with lower symmetry. The evaluated ϵ_β were estimated within a range between 4.2 and 15.4 nm, which is in good agreement with the powder SEM images (Figure 5).

As expected, the ϵ_β is increasing with the annealing temperature. These results agree with high-resolution transmission electron microscopy (HRTEM) and XRD data on thin film reported in ref 2. In fact, our previously obtained HRTEM images of the films have shown a broad scale of differently sized nanodomains ranging between 1 and 9 nm, the ϵ_β increasing also with the annealing temperature. This point has been confirmed by the SEM images (Figure 5) of the powder.

Above the dissociation temperature of ammonia, the optical transmission spectra are progressively red-shifted with increasing nitriding temperature. As observed in Figure 6, the progressive N^{3-}/O^{2-} anionic substitution gives the possibility to tune the absorption edge position by varying the nitridation temperature. This red shift is directly related to the nitrogen content determined by LECO apparatus (Table 1) and coincides with the observation generally made for micrometer-sized nitrided oxide powders.[14]

In our previous papers,[2,10] the presence of N^{3-} was confirmed on colored thin film by XPS techniques (the N K-edge located at 396.1 eV proves the presence of oxynitrides). In addition, when raising the nitridation temperature, a new Ti(2) component

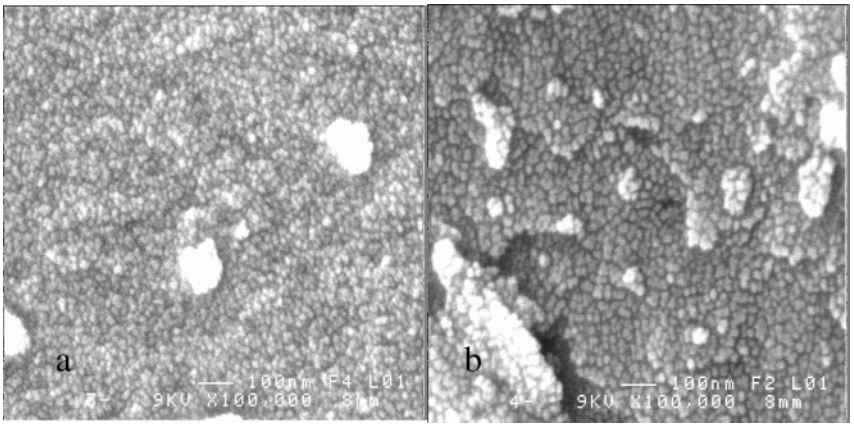

Figure 5. SEM images of nanosized powder annealed at 400 °C under air (a) and 700 °C under ammonia flow (b).

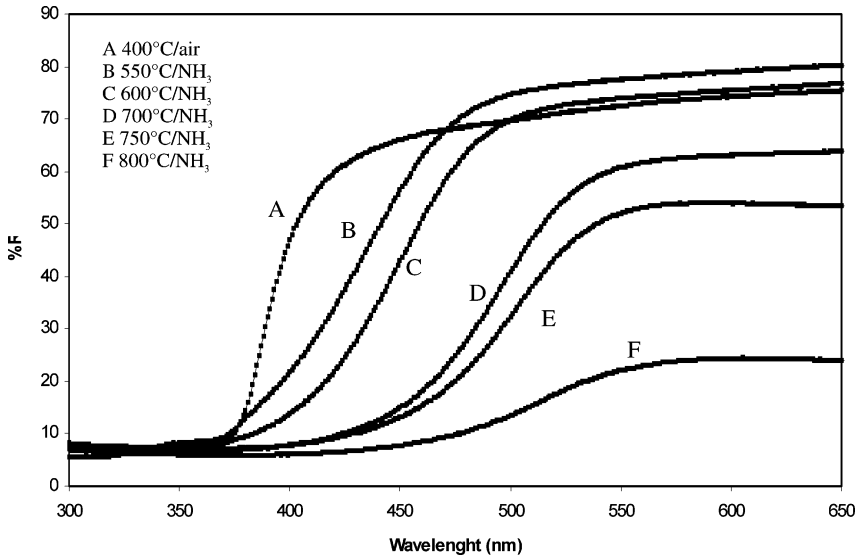

Figure 6. Changes in the optical transmission spectra of "ZnTiON" nanosized powders with increasing nitriding temperature.

appears at the low-energy side of the XPS−Ti spectra which is related to the nitrogen incorporation. This new component was attributed to Ti−N bounds.[2,10] In the present case of nanosized powders, preliminary XPS analysis of Zn and Ti reveals that after 1 h treatment under ammonia at 600 and 650 °C the Zn/Ti remains close to 1. Using all these results, a chemical formula could be proposed for the compounds annealed at 600 and 650 °C (Table 1), keeping the Zn/Ti ratio equal to 1. As an example, the chemical formula for the compound annealed at 650 °C could be written as $Zn_{1.33}Ti_{1.33}\square_{0.33}O_{3.49}N_{0.34}\square_{0.17}$ following ref 15. For higher temperature, analysis is in progress. Nevertheless we could expect some nonstable phases because LECO analyses show that, for temperatures higher than 800 °C, the nitrogen content decreases. The powder slightly becomes green-yellow, indicating a metal reduction process.[16] This phenomenon has been already observed for micrometer-sized powder oxynitrides—the nitrogen content reaches a maximum when the temperature is increased and then it decreases due to the volatilization or the reduction of metal.[15] As a result, the domain of existence of "ZnTiON" oxynitrides is limited in temperature (between 550 and 800 °C). Moreover, thermogravimetric measurement (temperature rate, 10 °C/min) shows that these oxynitrides are stable in air until 430 °C; a further increase of the weight indicates an oxidation process. Nevertheless, we notice that, thanks to our nanocolloid approach, pure oxynitride phases were obtained only after 1 h (only 15 min for 1 μm thick film) of annealing time under ammonia flow, whereas the classical nitridation process usually takes several hours.[15]

Conclusion

We are able to prepare new spinel oxynitride compounds with tunable band gap from white to yellow colors. A chemical formula is proposed for the compounds annealed at 600 or 650 °C, and it could be written as "$Zn_{1.33}Ti_{1.33}O_{4-3y}N_{2y}$". These compounds present promising semiconducting properties for potential gas sensing or sunscreen applications.

Acknowledgment. The authors thank N. Pontais for providing LECO analysis, F. Tessier for X-ray measurements facilities, Prof. Marchand for helpful discussion, and M. J. Le Lannic for supplying the SEM images.

References and Notes

(1) Klabunde, K. J. *Nanoscale Materials in Chemistry*; Wiley VCH: New York, 2001.

(2) Grasset, F.; Starukh, G.; Spanhel, L.; Ababou-Girard, S.; Su, D.; Klein, A. *Adv. Mater.* **2005**, *17* (3), 294.

(3) Schmidt, T.; Muller, G.; Spanhel, L. *Chem. Mater.* **1998**, *10*, 65.

(4) Hilgendorff, M.; Spanhel, L.; Rothenhäusler, C.; Müller, G. *J. Electrochem. Soc.* **1998**, *145*, 3632.

(5) Marchand, R.; Laurent, Y.; Guyader, J.; L'Haridon, P.; Verdier, P. *J. Eur. Ceram. Soc.* **1991**, *8*, 197.

(6) Spanhel, L.; Starukh, G.; Ababou-Girard, S.; Grasset, F. *Proceedings of 17th Workshop on Quantum Solar Energy Conversion (QUANTSOL 2005)*; Salzburg, Östrerreich, 2005.

(7) Lu, D.; Takata, T.; Saito, N.; Inoue, Y.; Domen, K. *Nature* **2006**, *440*, 295.

(8) Li, D.; Ohashi, N.; Hishita, S.; Kolodiazhnyi, T.; Haneda, H. *J. Solid State Chem.* **2005**, *178* (11), 3293.

(9) Audebrand, N.; Auffrédic, J. P.; Louër, D. *Chem. Mater.* **1998**, *10*, 2540.

(10) Grasset, F.; Spanhel, L.; Ababou-Girard, S. *Superlattices Microstruct.* **2005**, *38* (4−6), 300.

(11) Yang, J.; Swisher, H. *Mater. Charact.* **1996**, *37*, 156.

(12) Tomas, A.; Laruelle, P.; Dormann, J. L.; Nogues, M. *Acta Crystallogr.* **1983**, *C39*, 1615.

(13) Kim, H. T.; Kim, Y.; Valant, M.; Suvorov, D. *J. Am. Ceram. Soc.* **2001**, *84* (5), 1081.

(14) Diot, N.; Larcher, O.; Marchand, R.; Kempf, J. Y.; Macaudière, P. *J. Alloys Compd.* **2001**, *45*, 323.

(15) Louis dit Picard, C.; Merdrignac, O.; Guyader, J.; Laurent, Y. *J. Solid State Chem.* **1995**, *119*, 304.

(16) Orhan, E.; Tessier, F.; Marchand, R. *Solid State Sci.* **2002**, *4*, 1071.